Dimer-to-Monomer Transformation of Rhodamine 6G in Aqueous PEO−PPO−PEO Block Copolymer Solutions

R. Vogel,[†] M. Harvey,*[,‡] G. Edwards,[§] P. Meredith,[‡] N. Heckenberg,[‡] M. Trau,[†] and H. Rubinsztein-Dunlop[‡]

The Centre for Nanotechnology and Biomaterials and The Centre for Laser Science, The University of Queensland, Brisbane Qld 4072, Australia

Received June 11, 2001; Revised Manuscript Received November 5, 2001

ABSTRACT: To construct a viable dye-based microlaser, it is necessary to achieve very high dye concentrations in a solid matrix. Increased aqueous solubility of the laser dye Rhodamine 6G has been demonstrated in liquid and gel phases, using the triblock copolymer P123 as a surfactant. An increased monomer concentration and the suppression of aggregation of the dye molecules were observed using spectral absorption and fluorescence measurements. The micellation of P123 was studied using differential scanning calorimetry. The optical and thermal data suggest that this micellation process leads to a partitioning of Rhodamine 6G in solution and ultimately drives the equilibrium toward monomer retention. Results from a linear partitioning model support this hypothesis and are in qualitative agreement with the experimental data. These findings pave the way for higher concentrations of Rhodamine 6G to be used in aqueous-based dye lasers and also indicate how Rhodamine 6G could be used in solid-state microlaser systems.

Introduction

The aggregation of laser dye molecules such as Rhodamine 6G (R6G) in the form of dimers or higher aggregates quenches fluorescence and therefore degrades the lasing ability of laser dye systems. In aqueous solutions, the quenching process of R6G is due to the transfer of the excitation energy between monomers and aggregates[1−4] and to the very low quantum yield of R6G dimers.[5] However, the fluorescence quenching produced by the R6G monomer is negligible.

Dimerization comes about as the concentration of dye is increased beyond some critical value. In methanol and ethanol, R6G monomers are present alone up to concentrations on the order of 0.1 mol/L,[6] whereas in aqueous solutions, R6G begins to form dimers at concentrations as low as 1×10^{-5} mol/L.[6,7] In aqueous solutions, the R6G dimer consists of two dye molecules bridged by a water molecule. Because of the resulting fluorescence quenching, R6G in water is not able to exhibit lasing for concentrations greater than approximately 1×10^{-4} mol/L.[6,7]

Dimer-to-monomer transformations of some Rhodamine derivatives have been observed in micellar solutions of surfactants, for example, sodium dodecyl sulfate (SDS).[8] The same effect has been seen for R6G in sol gel silica films.[6] In this paper, it is demonstrated that P123 has the ability to suppress the aggregation of R6G by emulsifying the dye monomers and thus effectively partitioning the solution.

PEO20−PPO70−PEO20 (hereafter referred to by its trade name P123) consists of polyoxyethylene−polyoxypropylene−polyoxyethylene blocks. These PEO−PPO−PEO triblock copolymers are commonly referred to by the trade names Pluronics, Polaxamers, or Synperonics. They are used in industry for applications in cosmetic formulation, drug delivery,[9,10] the extraction of proteins,[11] corrosion protection,[12] and water-based paint.[13]

The family of PEO−PPO−PEO molecules are amphiphilic and surface-active, and they aggregate when in aqueous solution. Techniques such as nuclear magnetic resonance (NMR),[14,15] small-angle neutron scattering (SANS),[13,16−18] small-angle X-ray scattering (SAXS),[19,20] specific volume,[21,22] light scattering,[23−25] fluorescence spectroscopy,[26−28] UV/vis spectroscopy,[29] and differential scanning calorimetry (DSC)[30] have been applied to investigate their aggregation behavior. The PEO−PPO−PEO molecules self-aggregate by forming micelles with a hydrophobic core composed mainly of polyoxypropylene (PPO) segments and a corona composed mainly of the hydrophilic polyoxyethylene (PEO) segments.[31]

In comparison with normal carbon surfactants, which have a distinct critical micelle concentration (cmc), PEO−PPO−PEO systems aggregate over a range of concentrations. This behavior has been attributed to (i) polydispersity,[29] (ii) the existence of monomolecular micelles,[32] and (iii) changes in the size, shape, and polarity of the aggregates over this concentration range.[27]

Two of the most characteristic properties of aqueous PEO−PPO−PEO block copolymer solutions are their temperature-dependent micellation and gel formation.[29] The micellation can be explained by the change of the hydrophobic and hydrophilic tendency of PPO and PEO segments with temperature. For a given concentration of PEO−PPO−PEO monomers in aqueous solution, the dehydration of PPO segments with increasing temperature causes the aggregation of polymer molecules. The temperature at which this aggregation begins to occur is commonly termed the critical micelle temperature (cmt). With further increases in temperature, gelation is generally observed.[30] It has been shown by SANS that gelation occurs when the solution undergoes a phase transition from isotropic dispersed micelles to a body-centered-cubic (bcc) ordered liquid crystalline system.[17]

[†] The Centre for Nanotechnology and Biomaterials.
[‡] The Centre for Laser Science.
[§] Very Small Particle Company pty. ltd., P.O. Box 1022, Mt. Ommaney, Qld. 4074 Australia.
* To whom correspondence should be addressed: e-mail harvey@physics.uq.edu.au.

10.1021/ma010995l CCC: $22.00
Published on Web 02/09/2002

It has been previously shown that several dyes (e.g., pyrene,[26] sodium-2-(*N*-dodecylamino)naphthalene-6-sulfonate (C12NS),[27] 1,6-diphenyl-1,3,5-hexatriene (DPH),[29] benzopurpurine[33]) can be solubilized in different aqueous PEO−PPO−PEO solutions. In these studies, the effect on the dye of the solvation process was detected by fluorescence and UV/vis spectra, and additionally, cmc and cmt values were determined. In the study reported in this paper, the interaction between the dye dimer/monomer equilibrium in the aqueous phase and the emulsification of the monomer in P123 micelles was examined with a view to using the solid P123 gel as a laser gain material. This work was motivated by the desire to construct a micron scale dye laser system. Usually, dye lasers are based on solutions of dye in liquid (typically ethanol, methanol, or less commonly water) or on dye-doped solids such as sol−gel glasses.[34] To produce lasers scaled down to micron sizes, a liquid system is impractical, and one must resort to solid systems.[35,36] A suitable material for producing such microlasers would ideally have a very high concentration of gain material and little or no quenching of the fluorescence in the gain region, and it should be easy to shape into cavity structures. In addition to the preceding requirements, it is also desirable that the material be inexpensive, easy to work with, and not pose any particularly high risk to health or safety. P123, as a gel, satisfies all these requirements. It has been shown in the present work to provide a high ratio of monomers to dimers for R6G and hence has the potential to provide the high gain and low quenching needed for laser devices on micron scales.

Methods and Materials

Materials. The Pluronic compound P123 was a gift from BASF Corp. (Mount Olive, NJ). It was used without further purification. Laser grade Rhodamine 6G (R6G also known as Rhodamine 590) was purchased from Lambda Physics and also used without further purification. Water was obtained from a Milli-Q water purification system (Millipore), using distilled water as the input source.

P123 was dissolved in Milli-Q water to obtain 5, 10, 15, 25, and 30 wt % aqueous solutions. Subsequently, R6G was dissolved in these solutions at 1×10^{-3} mol/L concentration. This concentration of R6G was chosen because in pure aqueous solution the dye is certain to aggregate, and the absorption due to aggregates of the dye exceeds that due to the remaining dye monomers.

All samples were prepared at room temperature, and no adjustment was made to account for any effect which changes in temperature may have had on the concentration values. All concentrations stated in this paper are those of the as-prepared samples.

Differential Scanning Calorimetry. To determine the temperature range over which P123 undergoes the transition from distinct molecules in solution to micelles, differential scanning calorimetry was used. The DSC measurements were performed with a Pyris1 (Perkin-Elmer) device. Temperature scans were performed at a heating rate of 10 °C/min from −10 to 60 °C, using sample masses of approximately 10 mg. Results of the DSC measurements are presented in Table 1.

Absorption Spectroscopy (UV/vis). Absorption spectra were measured using a dual-beam Perkin-Elmer Lambda2 UV/vis spectrometer using a scanning rate of 96.0 nm/min. Cuvettes having path lengths of 0.3 and 0.5 mm were constructed by the Physics Department workshop at the University of Queensland by fixing aluminum spacers in between two glass slides and sealing the edges. All samples contained 1×10^{-3} mol/L concentration of R6G, 0.5 mm cuvettes were used for samples having 5, 10, and 15 wt % P123, and 0.3 mm cuvettes were used for samples having 20, 25, and 30 wt % P123. Temperature-controlled absorption measurements were conducted at a discrete range of temperatures (0, 2, 4, 6, 8, 10, 12, 14, 16, 18, 20, 25, and 30 °C). An uncovered, 20 L water bath was used as the temperature-controlled water source for these measurements. Prior to a measurement being made, the samples were left for 5 min in the water bath and held at the desired temperature so as to reach thermal equilibrium.

Table 1. DSC Results[a]

solution	T_{onset}	T_{peak}	T_{end}
P123 with 1×10^{-3} M Rh6G			
5 wt %	17.4	20.3	25.0
10 wt %	15.1	18.0	23.8
15 wt %	13.8	16.9	23.5
20 wt %	10.8	14.6	22.3
25 wt %	7.8	11.9	21.2
30 wt %	1.3	8.9	15.7
P123 only			
5 wt %	18.0	21.0	25.4
10 wt %	15.7	18.6	24.5
15 wt %	14.2	17.6	24.4
20 wt %	10.9	14.3	25.7
30 wt %	5.4	12.2	22.4

[a] T_{onset} is the onset temperature where micelles begin to form. T_{peak} is the peak temperature where micelle formation is occurring at the greatest rate. T_{end} is the end temperature, after which micelle formation is negligible.

Fluorescence Spectroscopy. Fluorescence spectra for the P123/R6G aqueous solutions were measured for the same range of temperatures. The measurements were performed with a Perkin-Elmer LS50B luminescence spectrometer equipped with a thermostatic cell unit, at a scan rate of 100 nm/min. Cuvettes having a 1 cm path length were used. All samples contained 1×10^{-3} mol/L concentration of R6G. The samples having 5, 10, 15, 20, and 25 wt % P123 were measured with the LS50B's excitation slit setting at 3.0 and its emission slit setting at 3.0. The sample with 30 wt % P123 was measured with the excitation slit set to 2.5 and the emission slit set to 2.5. In the same manner as for the absorption measurements, the samples were immersed in the temperature-controlled water bath for 5 min prior to each spectrum being measured. Emission intensity spectra were measured at wavelengths from 500 to 800 nm while an excitation wavelength of 450 nm was used.

Results and Discussion

Differential Scanning Calorimetry. DSC was carried out on samples prepared as detailed above to determine the temperature range over which the micellation process occurred for a given concentration of P123. The formation of micelles in P123 is an endothermic process, so the heat flow into the sample during micellation was a measure of the rate at which micelles were formed. The DSC data provided a means by which to determine the temperature range over which P123 underwent the transition from disparate molecules in solution to micelles.[30]

Unlike many other surfactants, P123 does not exhibit a well-defined start or finish temperature for the formation of micelles in solution. To make quantitative statements about the temperatures associated with micellation, three temperature values were defined for each sample: onset temperature (T_{onset}), peak temperature (T_{peak}), and end temperature (T_{end}). The onset temperature indicates the position of the onset of the micellation process, and the peak temperature is the temperature at which the DSC signal was a maximum, indicating the peak of the micellation process. The end temperature was taken as a measure of the temperature at which the micellation process had completed. Results

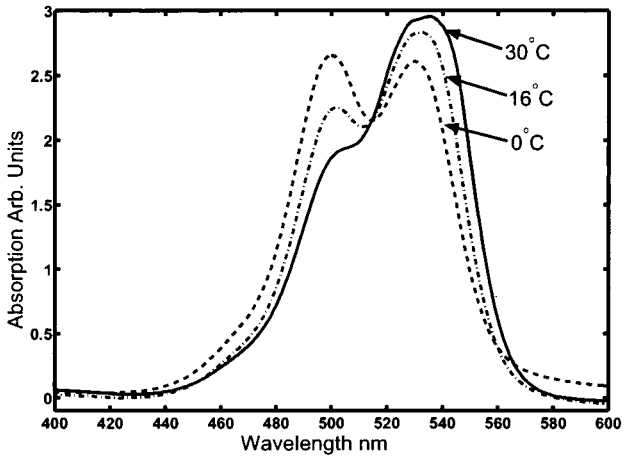

Figure 1. Absorption spectra at 0, 16 and 30 °C measured for a 5 wt % aqueous solution of P123 containing 1×10^{-3} mol/L R6G. The spectrum exhibits two peaks corresponding to the monomer and dimers of R6G in the solution.

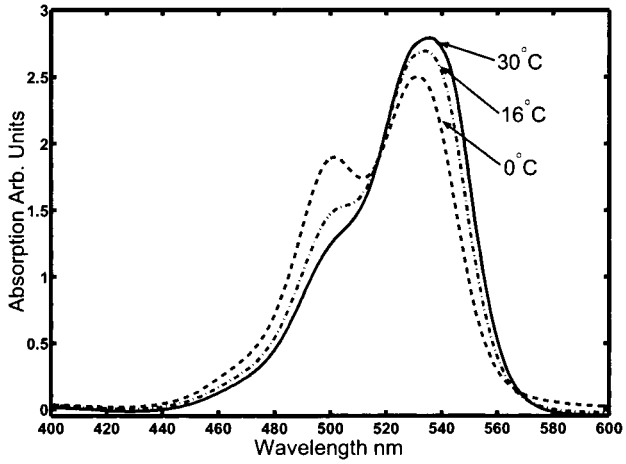

Figure 2. Absorption spectra for a 10 wt % aqueous solution of P123 containing 1×10^{-3} mol/L R6G, measured at 0, 16, and 30 °C.

of the DSC measurements are presented in Table 1. The measured values for the cmt of the P123 aqueous solutions are consistent with those reported by other authors.[30]

As the concentration of P123 was increased, the DSC data show that the micellation process moved to lower temperatures. The effect of this was to increase the number density of micelles in a solution at a given temperature. This is to be expected for a surfactant above its cmc and may be summarized as the cmc for P123 being inversely related to temperature.

P123 in aqueous solution will undergo further organization into liquid crystal phases (bcc and hexagonal) as the temperature of the solution is increased.[30] The heat flow associated with this transition was not observed in the present data, but the gelation of the samples indicated that such phase transitions had occurred. This leads to the conclusion that the energies associated with such further organization were small in comparison to those due to the formation of micelles.

Absorption Spectrometry. The absorption spectra for R6G in water exhibit two distinct maxima. These are clearly visible in Figure 1. The positions of these maxima were not observed to be influenced by the presence of P123 in the solution. One peak occurs at approximately 526 nm and the other at approximately 499 nm. It has been shown, by previous authors, that the longer wavelength peak is caused by absorption by free monomers of the dye and that the other is due to coupling between two dye molecules existing as a dimer.[29,40] The absorption spectra were observed to be independent of the temperature history of the sample.

It was assumed that, over the small temperature range investigated, the absorption cross sections of the Rhodamine monomers and dimers did not change. It was further assumed that any variation in the absorption peaks was due to changes in the number density of available absorbing species. It was found that the absorbers in this solution were mainly restricted to dye monomers and dimers. The removal of a dimer added two monomers, and vice versa. For all samples, when a change was observed in the magnitude of one of the peaks with temperature, a change in the opposite sense was observed in the other peak. An analysis of the magnitude of such changes produced an almost exactly two to one relationship between the removal of a dye aggregate and the introduction of monomers. This point is discussed in more detail later.

Figure 1 shows several spectra for a sample containing 5 wt % P123 and 1×10^{-3} mol/L R6G at various temperatures. At low temperatures, the dimer signal was slightly greater than that due to monomers. As the temperature was increased, the dimer signal fell and the monomer peak grew. Comparing this with the DSC data, it is clear that the temperatures over which the rate of change was greatest correspond to those over which the micelles were forming (i.e., between T_{onset} and T_{end}). Figure 2 shows the same effect for a sample having 10 wt % P123 and 1×10^{-3} mol/L R6G. Note that, for a given temperature, the relative dimer signal was lower in the 10 wt % solution than that observed for the 5 wt % solution. It was seen generally that with increasing polymer concentration the dimer signal was lower for a given temperature, which is consistent with the cmc changing inversely with temperature.

For the 20, 25, and 30 wt % samples, as the temperature was increased, the solution was observed to gel as it underwent a phase transition to what is believed to be a bcc liquid crystal phase.[30] There was no observed change in the absorption signal over the range of this phase transition.

There were two main effects observed in the absorption spectra:

1. For a fixed concentration of P123, as the sample temperature was increased, the absorption due to dimers decreased. This could be explained as follows: As the temperature in the P123 solution was raised, the polymer began aggregating into micelles and the presence of micelles facilitated the removal of monomers from the continuous aqueous phase. The removed monomers were thus partitioned in the micellar phase and still absorbed light in the same manner as those remaining in the aqueous phase. The R6G dimer consists of two R6G molecules linked by a water molecule, so dimers would not be expected to enter the micelles. Hence, the micelles would contain only monomers. To remain at equilibrium in the aqueous phase, dimers were converted into monomers, so the dimer signal kept falling (and the monomer signal rising) until no more micelles could be formed. At this point the number of micelles was static, and so no further change was observed in the absorption spectrum. This is illustrated in Figure 3.

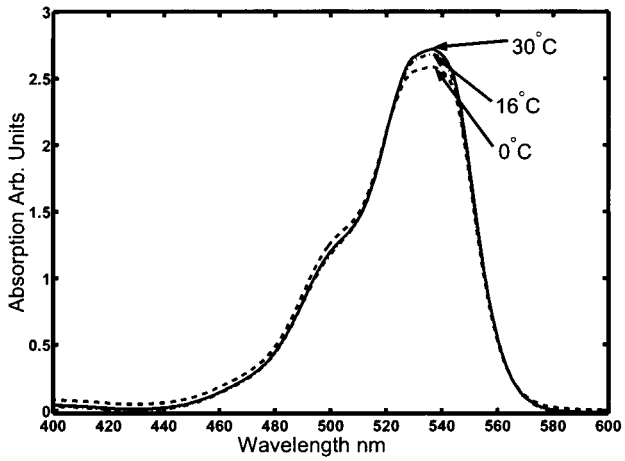

Figure 3. Absorption spectra measured at 0, 16, and 30 °C for a 30 wt % aqueous solution of P123 containing 1×10^{-3} mol/L R6G.

2. With increasing P123 concentration, at a fixed temperature, the dimer signal in the dye solutions decreased. The number of micelles in solution was approximately proportional to the concentration of the surfactant, and as the number of micelles increased, the dimer signal fell. If the micelles were partitioning the solution, then higher P123 concentrations should have exhibited a lower dimer signal as the ratio of micelle number to dye molecules was increased. This was indeed seen and is illustrated by comparing Figures 1−3. Eventually, a concentration was reached at which there were no further dimers available to be converted to monomers, and adding more P123 had no effect on the absorption spectrum.

Having proposed an explanation for the observed changes in the absorption spectra, it is possible to quantify these changes somewhat. In particular, an analysis of the absorption spectra obtained demonstrates that the dye aggregates are primarily dimers. This was established by an examination of the relative change in the absorption peaks, allowing for the different absorption cross sections exhibited by the monomer and dimer forms of the dye. For any sample, for which the Beer−Lambert approximation is valid, the following relationship holds for the absorption of light passing through the sample (assuming only monomers and dimers of the dye contribute to the absorption):

$$\frac{\Delta n_M}{\Delta n_D} = \frac{\Delta A_M(\lambda_M)\, \sigma_D(\lambda_D)}{\Delta A_D(\lambda_D)\, \sigma_M(\lambda_M)} = a \qquad (1)$$

Δn_M is the absolute change in the number of absorbing monomers, and similarly Δn_D is the absolute change in dimer number. $\Delta A_M(\lambda_M)$ and $\Delta A_D(\lambda_D)$ are the absolute changes in absorption due to monomers and dimers, respectively. $\sigma_M(\lambda_M)$ and $\sigma_D(\lambda_D)$ are the absorption cross sections at the wavelengths at which the absorption measurements are made. a is the average number of monomers produced by the removal of one dimer. If all the dye aggregates were dimers, then a would be two, indicating that for each aggregate removed there are two monomers added. To ensure that the Beer−Lambert approximation is valid, the peak absorption wavelengths for the monomer and dimer spectrum can be used.

$\Delta A_M(\lambda_M)$, $\Delta A_D(\lambda_D)$, λ_M, and λ_D were determined for all the samples examined experimentally by fitting two Gaussian curves to the measured data. The values determined for the band peaks were $\lambda_M = 497.4$ nm and $\lambda_D = 533.6$ nm. Taking $\sigma_M(\lambda_M) = 3.0 \times 10^{-16}$ cm^2 and $\sigma_D(\lambda_D) = 6.6 \times 10^{-16}$ cm^2,[42] the data collected for 156 cases produced a value for a of 2.2 ± 0.2 at the 95% confidence level. While this is in good agreement with the expected result,[41] the slightly elevated value may indicate that there are some small numbers of higher order dye aggregates in the solution which were also converted to monomers.

An important result from the absorption spectra measurements is that the dimers are actually being transformed into monomers and not just prevented from interacting with the light. This indicates that the changes in the fluorescence spectra, reported below, are due to changes in the number of monomers and not simply a reduction of the quenching in the solution.

Fluorescence Spectrometry. Fluorescence spectra were obtained for R6G in aqueous solution using an excitation source centered at 450 nm and having a fwhm of 7 nm. The Rhodamine monomer was observed to have a fluorescence peak at approximately 560 nm, and the dimer had a peak at a longer wavelength, approximately 611 nm. The spectra gathered were a sum of the monomer and dimer emission, although the contribution from dimers was expected to be negligible due to the low quantum efficiency of dimer fluorescence. Because of the high concentrations of dye in the samples being examined, it was expected that the fluorescence spectra would exhibit self-absorption effects. The impact of these effects would be to shift the fluorescence peak to just outside the absorption band, and this is precisely what was observed.[43]

Two effects were expected to demonstrate that the dimers in solution with P123 were being converted into monomers.

1. The removal of dimers would tend to cause the number of monomers having a solvation environment associated with the P123 micelles to increase. Such a change in environment would then be expected to be manifested as some change in the monomer fluorescence.[44] In the experimental study, the maximum of the summed fluorescence spectrum was observed to move toward 590 nm. An additional factor, which could have contributed to this, was the removal of any dimer fluorescence. As this shift, for either of the reasons presented, depends on the increased presence of dye monomers, it could not go beyond the limiting case of pure monomer self-absorption (i.e., 590 nm).

2. The increase in monomer concentration would see the magnitude of the monomer fluorescence peak increase.

These two effects were observed. Figure 4 shows fluorescence spectra obtained for a sample containing 5 wt % P123 and 1×10^{-3} mol/L R6G at several temperatures. At low temperatures, the magnitude of the emission was low, and the peak occurred at approximately 609 nm. As the temperature was raised, the wavelength at which the peak intensity was observed moved toward 590 nm and the magnitude of the emission peak increased.

Figure 5 shows the temperature dependence of the fluorescence peak intensity for various P123 concentrations. The data recorded were independent of the direction of the temperature variations. The DSC data presented in Table 1 have been overlayed on the graphs in Figure 5. It can be seen that changes in the fluorescent output of the material were greatest over the

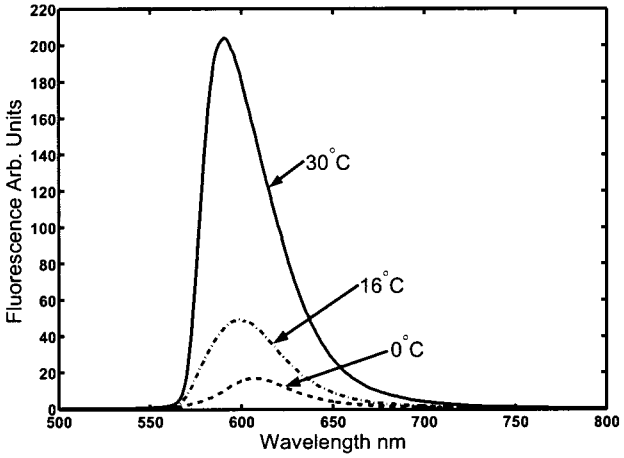

Figure 4. Fluorescence spectra measured at 0, 16, and 30 °C for a 5 wt % aqueous solution of P123 containing 1×10^{-3} mol/L R6G.

temperature range in which micellation of the P123 was observed by DSC. Importantly, for the case having no P123 in the solution, there was no systematic change in the magnitude of the fluorescence peak with temperature.

At low concentrations of P123 (<20 wt %), the fluorescent output of each sample began increasing at the temperature corresponding to the onset of micelle formation, T_{onset}, for that sample. Once again, this can be attributed to the dimers being converted into monomers as a result of the partitioning of the solution by the P123 micelles. Beyond the temperature corresponding to the end of the micelle forming process, T_{end}, there should be no production of additional micelles, and hence the monomer concentration does not change further. Consequently, as can be seen in Figure 5, there is no further change in the magnitude of the emission peak.

At higher concentrations of P123, the relationship between the onset of micelle formation and changes in the fluorescence spectrum was not as obvious. This was due to the rapidity with which the higher concentration of P123 formed a sufficient number of micelles to effectively remove all the available dimers. Even though micelles were still forming, there was no change in the spectrum beyond this point. The sample containing 30 wt %, shown in Figure 5, illustrates this point well. There was almost no change in the output as the temperature increased due to all the available dimers having been removed at low temperatures.

Figure 6 shows the temperature dependence of the wavelength at which the peak fluorescence intensity was measured for various P123 concentrations. As more monomers were made available, the position of the peak should have moved toward the value for the monomer alone. This can be seen in Figure 6, where the DSC results have been overlayed. It can indeed be seen that the changes occur at temperatures corresponding to the formation of micelles. Again, for the case having no P123 in the solution, there is no systematic change in the peak wavelength with temperature. These results are in good agreement with those for the fluorescence intensity discussed previously. At low concentrations of P123 (<20 wt %) the samples showed a change in peak wavelength toward 590 nm. Rapid changes were seen to occur between T_{onset} and T_{end}, indicating the role of micelles in the deaggregation of dimers. At higher P123 concentrations virtually no change was seen in the peak wavelength for reasons discussed above.

For several of the samples the solution was seen to gel as it underwent, what was presumed to be, a phase transition to a bcc liquid crystal phase.[30] There was no observed change in the fluorescence signal over the range of this phase transition. This is suggestive that the dye monomers were located away from the surface of the P123 micelles.

Partition Model. Above its cmt, P123 forms micelles and partitions the solution into two regions: the external, continuous aqueous phase and the internal micellar phase. It has been suggested that the dye molecules as monomers will associate with the hydrophobic chain on the surfactant[39] and then be included in micelles as they form, effectively removing these dye molecules from the aqueous phase. Inside the micelles, the hydrophobic cores are expected to provide an environment very different from the aqueous phase outside and thus inhibit (or even prevent) the formation of dimers, which consist of monomers linked by a water molecule.

R6G monomers in solution are in equilibrium with the dimers, and there is some equilibrium mole fraction reflecting this process.

$$\frac{M_{aq}}{R_{aq}} = K_{R,aq} \tag{2}$$

$$\frac{M_{mic}}{R_{mic}} = K_{R,mic} \tag{3}$$

where M is the number of monomers of R6G and R is the total number of R6G molecules in the solution. K_R is the mole fraction of R6G existing as monomers. The subscript "aq" implies the species is in the aqueous phase, and "mic" implies the species is in the micelle phase.

Applying conservation of mass yields

$$R_{aq} + R_{mic} = R_{in} \tag{4}$$

where R_{in} is the total number of R6G molecules initially placed in the solution.

It was seen from DSC measurements that the process of micelle formation was temperature-dependent, with a start and a finish temperature T_{onset} and T_{end}, respectively. Between T_{onset} and T_{end} the rate of micelle formation is not constant. The following expression implicitly accounts for any changes in the rate of micelle formation:

$$AS(T) + C(T_{end}) + \delta C(T) = P_{in} \tag{5}$$

where A is the aggregation number for P123 micelles, $S(T)$ is the number of micelles as a function of temperature T, and $C(T_{end})$ is the critical micelle number (cmc $\times$ volume) for P123 at the end temperature. This is the number of free surfactant molecules in solution at the end temperature. $\delta C(T)$ is the number of P123 molecules that would form into micelles at temperature T_{end} but have not due to the temperature being less than T_{end}. This then reflects the change in the critical micelle number with temperature (i.e., the change in the number of free surfactant molecules). P_{in} is the total number of P123 molecules. The effect of temperature on the formation of micelles is accounted for in $C(T_{end}) + \delta C(T)$. The only independent variable in the above

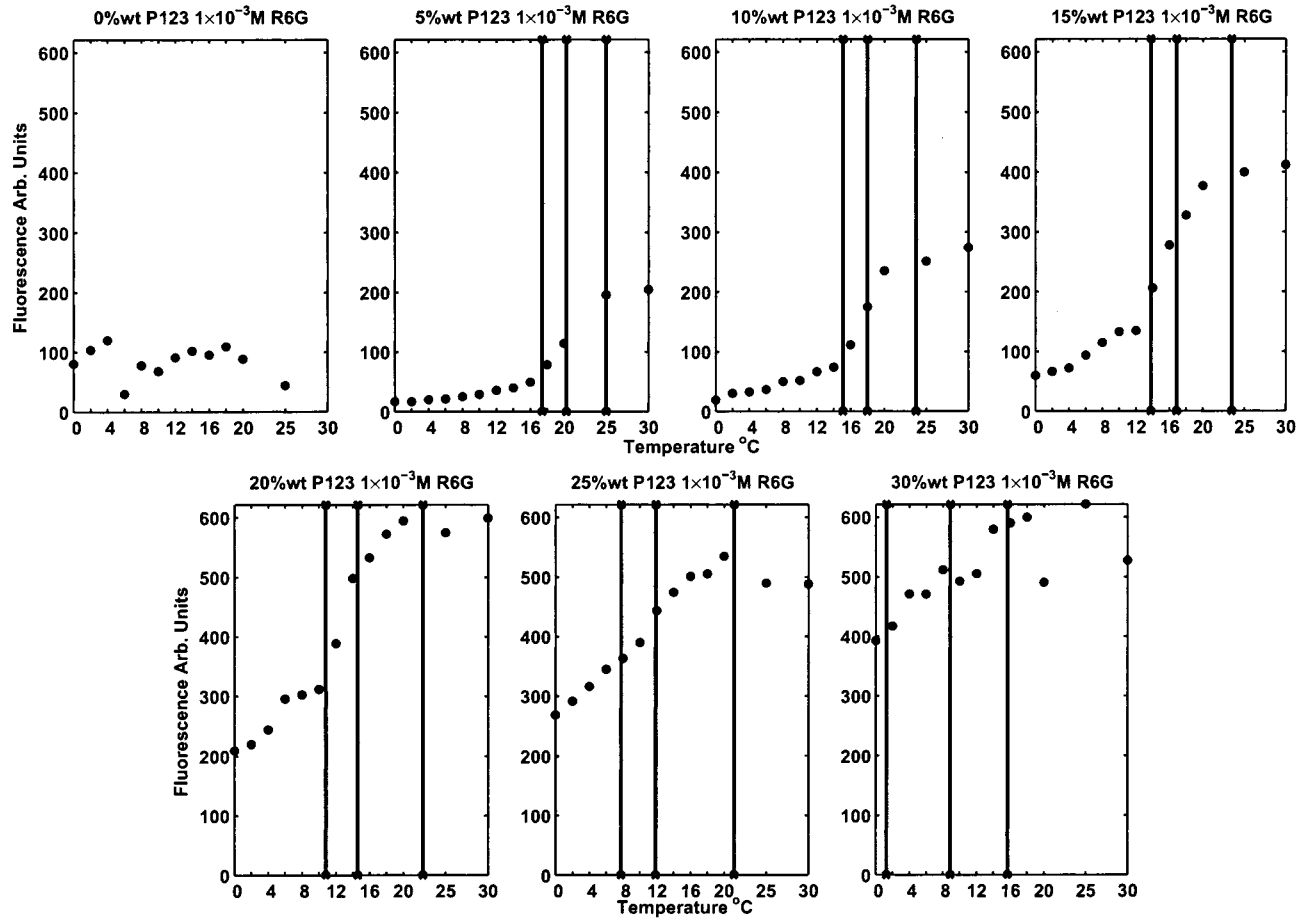

Figure 5. Peak fluorescence output as a function of temperature is shown for the seven concentrations of P123 in aqueous solution which were investigated. The vertical lines indicate the measured values of (from left to right) T_{onset}, T_{peak}, and T_{end}.

expression is $\delta C(T)$. It may be assumed, on the basis of the DSC results, that no micelles have formed at temperatures below T_{onset} and that no further micelles form for temperatures above T_{end}. From this it follows that upper and lower limits may be set on the value of $\delta C(T)$:

$$\delta C(T \leq T_{onset}) = P_{in} - C(T_{end}) = \text{constant} \quad (6)$$

$$\delta C(T \geq T_{end}) = 0 \quad (7)$$

At equilibrium, the following holds:

$$\frac{AS(T)}{P_{in} - C(T_{end})} = K_P(T) \quad (8)$$

where $K_P(T)$ is the equilibrium mole fraction of P123 molecules existing as micelles at some temperature T; the effect of $\delta C(T)$ is contained in $K_P(T)$. The definition of $C(T_{end})$ ensures the denominator of this expression will never be zero.

Assuming that the average dye molecule population in micelles is constant, n, the number of micelles and the number of R6G molecules inside micelles are related:

$$M_{mic}(T) = nS(T) \quad (9)$$

The total number of R6G monomers in the solution as a function of temperature is then

$$M_{aq} = K_{R,aq}R_{in} + \frac{n}{A}(K_{R,mic} - K_{R,aq})K_{P123}(T)(P_{in} - C(T_{end})) \quad (10)$$

For the model presented above, only three parameters are available for experimental control: P_{in}, R_{in}, and T. Figure 7 shows a series of absorption spectra predicted by the model presented here. To produce these curves, the absorption cross sections for the monomer and dimer peaks were used to relatively scale a pair of Gaussian curves. The widths of the Gaussians were obtained by fitting to experimental data. The predicted spectra were then produced by summing these two Gaussians, each scaled by the number of monomers or dimers predicted. The model parameters used for the spectra in Figure 7 are the same as those used for the experiments that produced the curves in Figure 1. Comparing Figures 1 and 7, this model is seen to be in in good agreement with the experimental data. The quantitative accuracy of this model, as applied in Figure 7, is limited by a number of factors. The most significant limitation is the use of a Gaussian curve to approximate the shape of the absorption spectrum for the monomers and dimers. The real spectral features are significantly more complicated than this, but the use of Gaussian curves greatly simplifies the calculation and still serves to illustrate the dynamics of the system.

The main results of applying this model are the following: (i) Partitioning of the solution, by micelle formation, leads to an increase in the number of

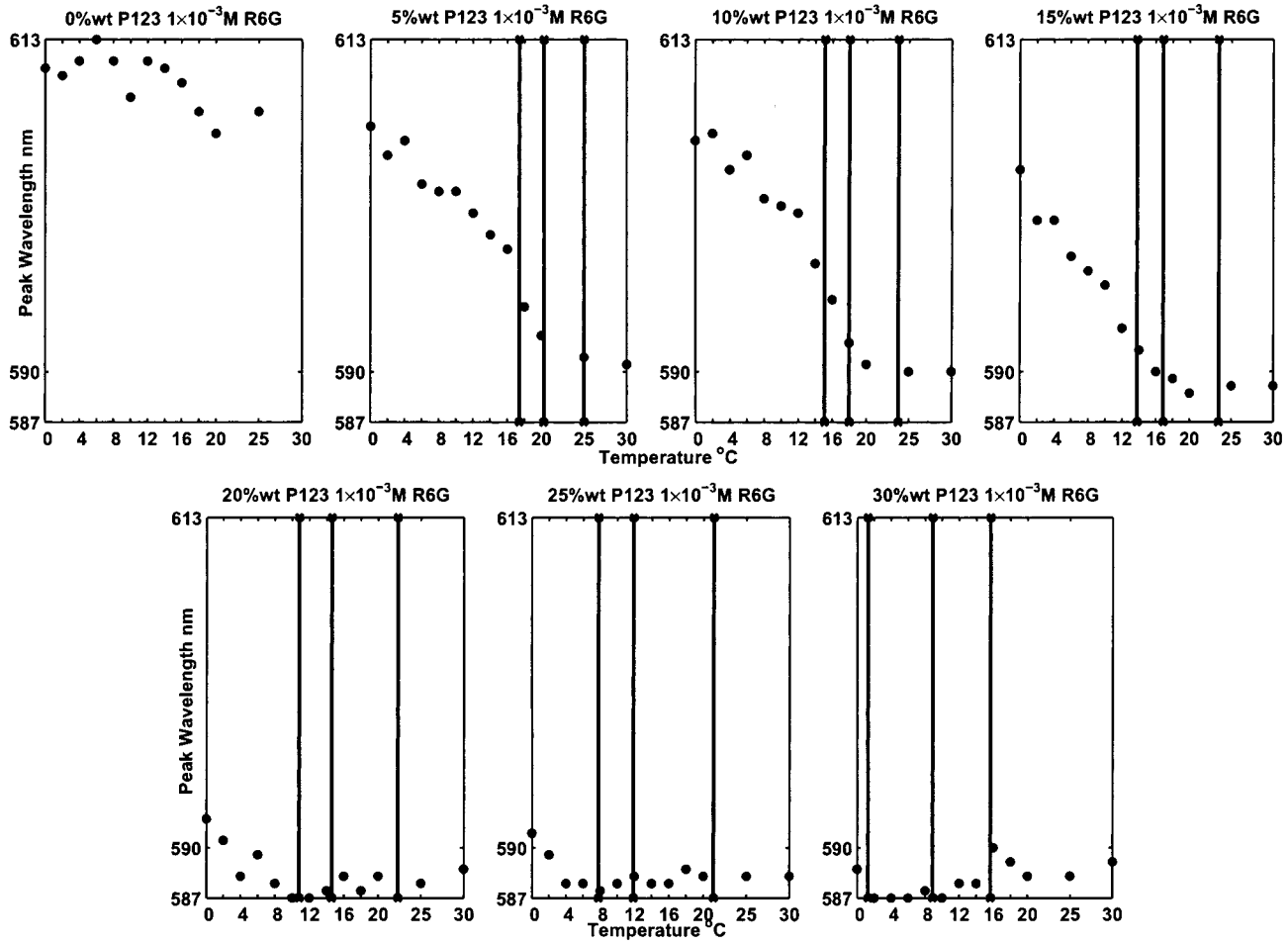

Figure 6. Wavelength at which the peak fluorescence was observed is plotted as a function of temperature for the seven concentrations of P123 in aqueous solution which were investigated. The vertical lines indicate the measured values of (from left to right) T_{onset}, T_{peak}, and T_{end}.

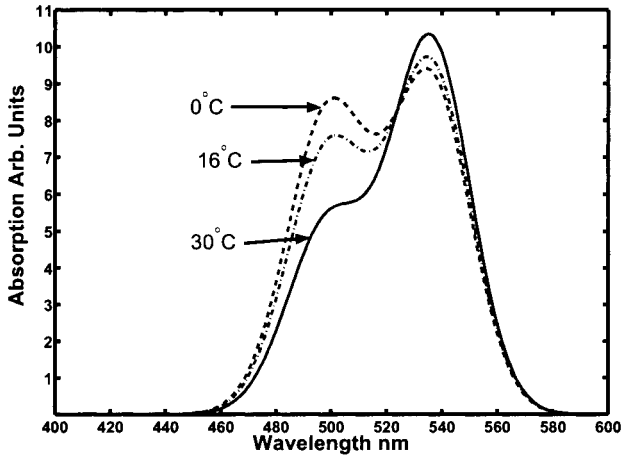

Figure 7. Theoretical absorption spectra generated by the partition model presented in the text. The model parameters match the experimental parameters used to generate the spectra in Figure 1.

monomers. (ii) Temperature-dependent changes in the absorption and fluorescence spectrum of this system are caused by the change of cmc with temperature. (iii) Dye aggregates are converted into monomers with a ratio of effectively 1:2, confirming that the main aggregate form of R6G is dimerization.

Conclusion

The presence of P123, in aqueous solution, with R6G was seen to produce a temperature-dependent enhancement of the monomer absorption consistent with dimers being converted to monomers and an increase in fluorescence output by an order of magnitude or more. These changes were most likely caused by the conversion of R6G dimers into monomers. This was further confirmed by calculating the aggregation number for the dye aggregates on this basis and finding good agreement with values produced by other authors. DSC measurements confirmed that the temperature ranges over which such enhancements occur correspond to those over which P123 forms micelles. Hence, P123 micellation is considered to be the primary cause of the observed increases in monomer concentrations.

Based on the hypothesis that the formation of micelles resulted in a partitioning of the solution, a simple model has been developed. Tracking the changes of the equilibrium values in each of the partition environments, this model seems to be in good agreement with the observed experimental spectra.

Additionally, the observation of clear start and end points for the changes in the fluorescence and absorption spectra of R6G as P123 micelles form leads to the suggestion of a novel means to determine the aggregation number for P123. To do this, the concentration of P123 at a fixed temperature is increased in a sample

having a well-determined concentration of dye until no further change is measured in the fluorescence and/or absorption spectrum. At this point the ratio of polymer to dye molecules is the aggregation number of P123. If the polymer is not monodisperse, a correction needs to be made.

Stimulated emission and whispering gallery laser modes in micron-scaled devices, using dyes for gain, have been reported recently.[36−38] Now that the formation of R6G dimers in aqueous solutions can be successfully controlled by the inclusion of P123, this material stands as a good candidate for producing laser action from such solid, micron-scaled devices. The present work may also shed some light on the origin of low-threshold effects seen by other workers.[35]

References and Notes

(1) Arbeloa, F. L.; Ojeda, P. R.; Arbeloa, I. L. *J. Chem. Soc, Faraday Trans.* **1988**, *84*, 1903−1912.
(2) Bojarski, C.; Obermueller, G. *Acta Phys. Pol., A* **1976**, *50*, 389−392.
(3) Grawoska, E.; Tyrzyk, J.; Bojarski, C. *Acta Phys. Pol., A* **1980**, *57*, 753−759.
(4) Levshin, V. L.; Baranova, E. G. *Opt. Spectrosc.* **1959**, *6*, 31−36.
(5) Penzkofer, A.; Leupacher, W. *J. Lumin.* **1987**, *37*, 61−72.
(6) Innocenzi, P.; Kozuka, H.; Yoko, T. *J. Non-Cryst. Solids* **1996**, *201*, 26−36.
(7) Schäfer, F. P. *Topics in Applied Physics*; Dye Lasers Springer: Berlin, 1973; Vol. 1.
(8) Pal, P.; Zeng, H.; Durocher, G.; Girard, D.; Giasson, R.; Blanchard, L.; Gaboury, L.; Villeneuve, L. *J. Photochem. Photobiol. A: Chem.* **1996**, *98*, 65−72.
(9) Seijo, B.; Fattal, E.; Roblottreupel, L.; Couvreur, P. *Int. J. Pharm.* **1990**, *62*, 1−7.
(10) Suzuki, K.; Saito, Y.; Tokuoka, Y.; Abe, M.; Sato, T. *J. Am. Oil Chem. Soc.* **1997**, *74*, 55−59.
(11) Tani, H.; Saitoh, T.; Kamidate, T.; Kamataki, T.; Watanabe, H. *Anal. Sci.* **1997**, *13*, 747−751.
(12) Rangelov, S.; Mircheva, V. *J. Mater. Sci., Lett.* **1997**, *16*, 209−211.
(13) Mortensen, K. *J. Phys.: Condens. Matter* **1996**, *8*, A103−A124.
(14) Almgren, M.; Bahadur, P.; Jansson, M.; Li, P.; Brown, W.; Bahadur, A. *J. Colloid Interface Sci.* **1992**, *151*, 157−165.
(15) Scheller, H.; Fleischer, G.; Karger, J. *J. Colloid Polym. Sci.* **1997**, *275*, 730−735.
(16) Goldmints, I.; vonGottberg, F. K.; Smith, K. A.; Hatton, T. A. *Langmuir* **1997**, *13*, 3659−3664.
(17) Mortensen, K. J. *Z. Phys. IV* **1993**, *3*, C8, 157−160.
(18) Schmidt, G.; Richtering, W.; Lindner, P.; Alexandridis, P. *Macromolecules* **1998**, *31*, 2293−2298.
(19) Alexandridis, P.; Olsson, U.; Lindman, B. *Langmuir* **1998**, *14*, 2627−2638.
(20) Wu, G.; Ying, Q.; Chu, B. *Macromolecules* **1994**, *27*, 5758−5765.
(21) Wen, X. G.; Verrall, R. E. *J. Colloid Interface Sci.* **1997**, *196*, 215−223.
(22) Williams, R. K.; Simard, M. A.; Jolicoeur, C. *J. Phys. Chem.* **1985**, *89*, 178−182.
(23) Wen, X. G.; Verrall, R. E.; Liu, G. J. *J. Phys. Chem. B* **1999**, *103*, 2620−2626.
(24) Nolan, S. L.; Phillips, R. J.; Cotts, P. M.; Dungan, S. R. *J. Colloid Interface Sci.* **1997**, *191*, 291−302.
(25) Zhou, Z.; Chu, B. *J. Colloid Interface Sci.* **1988**, *126*, 171−180.
(26) Bohorquez, M.; Koch, C.; Trygstad, T.; Pandit, N. *J. Colloid Interface Sci.* **1999**, *216*, 34−40.
(27) Holland, R. J.; Parker, E. J.; Guiney, K.; Zeld, F. R. *J. Phys. Chem.* **1995**, *99*, 11981−11988.
(28) Nakashima, K.; Anzai, T. T.; Fujimoto, Y. *Langmuir* **1994**, *10*, 658−661.
(29) Alexandridis, P.; Holzwarth, J. F.; Hatton, T. A. *Macromolecules* **1994**, *27*, 2414−2425.
(30) Wanka, G.; Hoffmann, H.; Ulbricht, W. *Macromolecules* **1994**, *27*, 4145−4159.
(31) Wen, X.; Sikorski, M.; Khmelinskii, I. V.; Verrall, R. E. *J. Phys. Chem. B* **1999**, *103*, 10092−10097.
(32) Prasad, K.; Luong, T.; Florence, A.; Paris, J.; Vaution, C.; Seiller, M.; Puisieux, F. *J. Colloid Interface Sci.* **1979**, *69*, 225−230.
(33) Anderson, R. A. *Pharm. Acta Helv.* **1972**, *47*, 304−311.
(34) Knobbe, E. T.; Dunn, B.; Fuqua, P. D.; Nishida, F. *Appl. Opt.* **1990**, *29*, 2729−2733.
(35) Yang, P.; Wirnsberger, G.; Huang, H. C.; Cordero, S. R.; McGehee, M. D.; Scott, B.; Deng, T.; Whitesides, G. M.; Chmelka, B. F.; Buratto, S. K.; Stucky, G. D. *Science* **2000**, *287*, 465−467.
(36) Wirnsberger, G.; Stucky, G. D. *Chem. Mater.* **2000**, *12*, 2525−2527.
(37) Vietze, U.; Kraus, O.; Laeri, F.; Ihlein, G.; Schueth, F.; Limburg, B.; Abraham, M. *Phys. Rev. Lett.* **1998**, *81*, 4628−4631.
(38) Braun, I.; Ihlein, G.; Laeri, F.; Noeckel, J. U.; Schulz-Ekloff, G.; Schueth, F.; Vietze, U.; Wess, O.; Woehrle, D. *Appl. Phys. B* **2000**, *70*, 335−343.
(39) Fischer, M.; Georges, J. *Spectrochim. Acta A* **1997**, *53*, 1419−1430.
(40) Antonov, L.; Gergov, G.; Petrov, V.; Kubista, M.; Nygren, J. *Talanta* **1999**, *49*, 99−106.
(41) Selwyn, J. E.; Steinfeld, J. I. *J. Phys. Chem.* **1972**, *76*, 762−774.
(42) Lu, Y.; Penzkofer, A. *J. Chem. Phys.* **1986**, *107*, 175−184.
(43) Ganiel, U.; Neumann, G.; Treves, D. *IEEE J. Quantum Electron.* **1975**, *QE-11*, 881−891.
(44) Hungerford, G.; Suhling, K.; Ferreira, J. *J. Photochem. Photobiol.* **1999**, *129*, 71−80.

MA010995L